

# UC San Diego

## UC San Diego Previously Published Works

### Title

Benzothiazole Amphiphiles Ameliorate Amyloid  $\beta$ -Related Cell Toxicity and Oxidative Stress

### Permalink

<https://escholarship.org/uc/item/9cj63103>

### Journal

ACS Chemical Neuroscience, 7(6)

### ISSN

1948-7193

### Authors

Cifelli, Jessica L  
Chung, Tim S  
Liu, Haiyan  
et al.

### Publication Date

2016-06-15

### DOI

10.1021/acscemneuro.6b00085

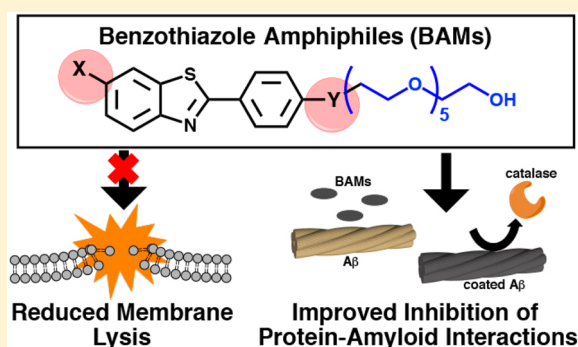
Peer reviewed

# Benzothiazole Amphiphiles Ameliorate Amyloid $\beta$ -Related Cell Toxicity and Oxidative Stress

Jessica L. Cifelli,<sup>†</sup> Tim S. Chung,<sup>†</sup> Haiyan Liu,<sup>‡</sup> Panchika Prangkiyo,<sup>‡</sup> Michael Mayer,<sup>‡</sup> and Jerry Yang<sup>\*,†</sup><sup>†</sup>Department of Chemistry and Biochemistry, University of California, San Diego, 9500 Gilman Drive, La Jolla, California 92093-0358, United States<sup>‡</sup>Department of Biomedical Engineering, University of Michigan, 1101 Beal Avenue, Ann Arbor, Michigan 48109, United States**S** Supporting Information

**ABSTRACT:** Oxidative stress from the increase of reactive oxygen species in cells is a common part of the normal aging process and is accelerated in patients with Alzheimer's disease (AD). Herein, we report the evaluation of three benzothiazole amphiphiles (BAMs) that exhibit improved biocompatibility without loss of biological activity against amyloid- $\beta$  induced cell damage compared to a previously reported hexa(ethylene glycol) derivative of benzothiazole aniline (BTA-EG<sub>6</sub>). The reduced toxicity of these BAM agents compared to BTA-EG<sub>6</sub> corresponded with their reduced propensity to induce membrane lysis. In addition, all of the new BAMs were capable of protecting differentiated SH-SY5Y neuroblastoma cells from toxicity and concomitant oxidative stress induced by AD-related aggregated A $\beta$  (1–42) peptides. Binding and microscopy studies support that these BAM agents target A $\beta$  and inhibit the interactions of catalase with A $\beta$  in cells, which, in turn, can account for an observed inhibition of A $\beta$ -induced increases in hydrogen peroxide in cells treated with these compounds. These results support that this family of benzothiazole amphiphiles may have therapeutic potential for treating cellular damage associated with AD and other A $\beta$ -related neurologic diseases.

**KEYWORDS:** Alzheimer's disease (AD), A $\beta$ , oxidative stress, catalase, benzothiazoles



Oxidative damage due to an imbalance of production and degradation of reactive oxygen species (ROS) in neurons is a normal part of the aging process<sup>1</sup> and is accelerated in Alzheimer's disease (AD).<sup>2–4</sup> In particular, elevated levels of ROS are found associated with regions of high accumulation of amyloid- $\beta$  (A $\beta$ ) in the brains of patients with AD.<sup>5</sup> The brain is highly susceptible to oxidative stresses due to slow regeneration, high oxygen consumption, and low levels of antioxidants,<sup>6,7</sup> making it important to develop methods to combat oxidative stress in AD.

Recent evidence supports a detrimental interaction between aggregated forms of A $\beta$  and the antioxidant enzyme catalase.<sup>8</sup> Catalase plays an important role in maintaining normal levels of ROS by catalyzing the degradation of hydrogen peroxide (H<sub>2</sub>O<sub>2</sub>).<sup>1</sup> The interaction between A $\beta$  and catalase causes deactivation of catalase and subsequently an increase in cellular levels of H<sub>2</sub>O<sub>2</sub>.<sup>8,9</sup> Compounds that can inhibit A $\beta$ -catalase interactions in cells may, therefore, represent a new therapeutic strategy for treatment of AD.

We previously reported the design, synthesis, and evaluation of two oligo(ethylene glycol) derivatives of benzothiazole aniline (BTA), BTA-EG<sub>6</sub> and BTA-EG<sub>4</sub>, which exhibited a variety of advantageous properties for the potential treatment of neurodegenerative diseases such as AD.<sup>8,10</sup> These properties include the capability to 1) bind to aggregated forms of several

different amyloidogenic proteins or peptides in the nanomolar range,<sup>11</sup> 2) cross the Blood Brain Barrier (BBB),<sup>12</sup> 3) protect cells from toxicity and oxidative stress induced by aggregated A $\beta$  peptides,<sup>8</sup> 4) decrease A $\beta$  levels *in vivo*,<sup>12</sup> and 5) improve memory and learning in a mouse model for AD.<sup>10,12</sup> The *in vivo* properties of these BTA-EG<sub>x</sub> compounds suggest that they may be capable of slowing down cognitive decline associated with AD. While the therapeutic potential of this class of compounds is attractive, these BTA-EG<sub>x</sub> compounds exhibited some toxicity in neuroblastoma cells at concentrations below 100  $\mu$ M, which we showed correlated with their capability to form pores in membranes and induce membrane lysis.<sup>13</sup>

In order to improve the biocompatibility of this class of compounds, we synthesized and evaluated the toxicity and membrane pore-forming capability of three benzothiazole amphiphiles (BAMs), with structures that differed from BTA-EG<sub>6</sub> through alterations made to the hydrophobic core. Here we show that these new BAM agents exhibited a reduced propensity to induce ion channel-like transmembrane current fluctuations in planar lipid bilayers, a reduction in membrane lysis activity, and overall lower toxicity to differentiated

Received: March 17, 2016

Accepted: April 7, 2016

Published: April 7, 2016

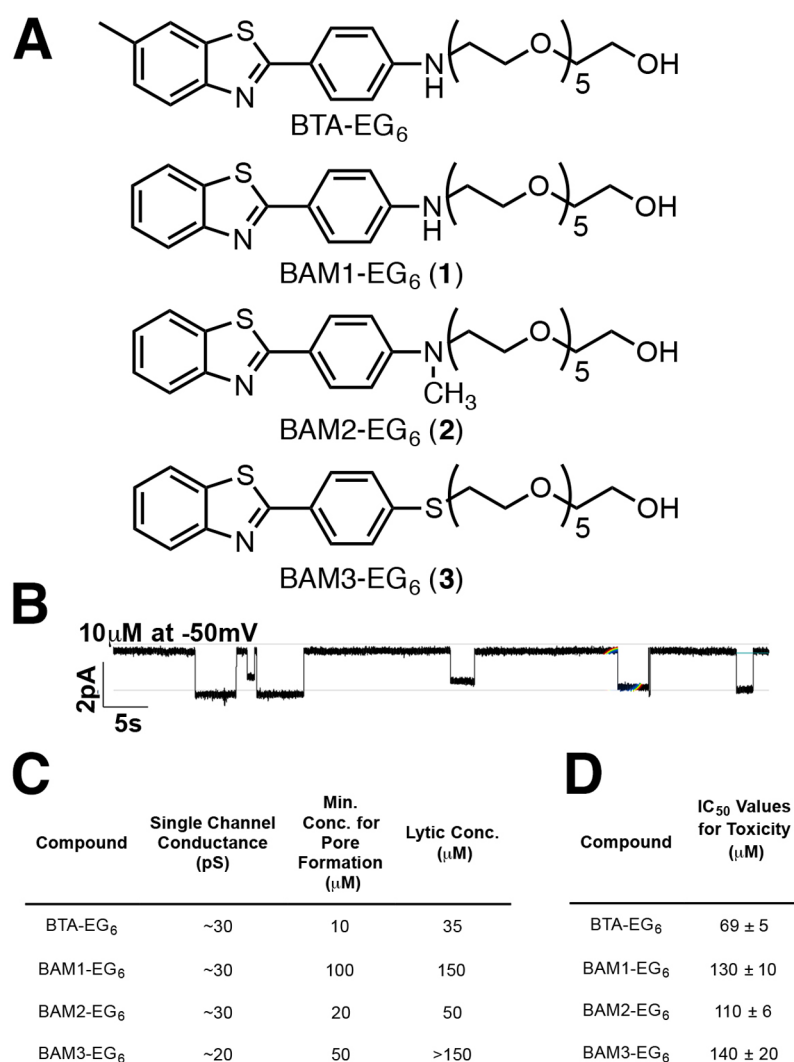


**Figure 1.** Evaluation of the lytic and toxic properties of BAMs 1–3 and BTA-EG<sub>6</sub>. (A) Chemical structures of BTA-EG<sub>6</sub> and BAMs 1–3. (B) Representative current versus time trace from single ion channel recordings of BTA-EG<sub>6</sub> in a planar lipid bilayer composed of DiPhyPC lipids. (C) Summary of ion channel data for BTA-EG<sub>6</sub> and BAMs 1–3. Minimum concentration for pore formation is defined as the concentration where transmembrane fluctuations were observed at a frequency above 0.05 per minute. (D) Toxicity data for BTA-EG<sub>6</sub> and BAMs 1–3 in differentiated SH-SY5Y neuroblastoma cells.

neuroblastoma cells. In addition, all new BAM derivatives retained their capability to protect cells against A $\beta$ -induced toxicity and oxidative stress. Finally, these BAMs were found to decrease colocalization and binding of catalase to aggregated A $\beta$  peptides in cells. Thus, the cytoprotective effects of these compounds support a previously proposed mechanism of formation of protein-resistive coatings on aggregated A $\beta$  peptides, leading to inhibition of catalase-amyloid interactions that would otherwise promote cellular increases in H<sub>2</sub>O<sub>2</sub>. These BAM compounds, thus, represent a new family of potential anti-A $\beta$  therapeutics that may have utility as part of a combined therapeutic regiment for AD.

In order to further develop benzothiazole amphiphiles as potential therapeutics for AD, we considered whether small variations in the structure of the BTA-EG<sub>x</sub> compounds could increase their therapeutic window.<sup>14</sup> Toward this end, we previously reported that BTA-EG<sub>4</sub> could form cation-selective pores in planar lipid bilayers.<sup>13</sup> The concentration required to observe ion channel-forming activity in membranes was roughly the same as the concentration required to observe cytotoxicity

of the compounds in human SH-SY5Y neuroblastoma cells (IC<sub>50</sub>  $\sim$  60  $\mu$ M), suggesting ion pore-mediated lysis of cells as a potentially significant factor for the observed toxicity<sup>15</sup> of the BTA-EG<sub>x</sub> compounds at micromolar concentrations.<sup>13</sup> Hence, we hypothesized that altering the hydrophobic core of these molecules would decrease their energetic driving force to partition into membranes, thereby reducing their ion channel forming capabilities and concomitant toxicity.

To test this hypothesis, we used BTA-EG<sub>6</sub> as the lead compound for the rational design of three Benzothiazole Amphiphile<sup>16</sup> (BAM) derivatives (Figure 1a, see Scheme 1 in the SI for details of the syntheses). Here, we presume the benzothiazole core is required to impart efficient binding to aggregated A $\beta$  peptides. We, therefore, examined the effects on membrane activity of the following three changes to the periphery of the benzothiazole core of BTA-EG<sub>6</sub>: 1) removal of the 6-methyl group (as in BAM1-EG<sub>6</sub>), 2) addition of a methyl group to the aniline nitrogen (as in BAM2-EG<sub>6</sub>), and 3) replacement of the aniline nitrogen with a sulfur group (as in BAM3-EG<sub>6</sub>).

Since we previously found that toxicity corresponded with the ion-channel forming properties of BTA-EG<sub>6</sub>,<sup>13</sup> we first examined the ion channel-forming properties of compounds 1–3 compared to BTA-EG<sub>6</sub> in bilayer lipid membranes (BLMs). Similar to previous studies, we observed ion channel-like events in these cell free bilayer experiments at mid to high micromolar concentrations of the compounds (Figure 1b, also see Figures S1–S3 in the SI). Importantly, while BTA-EG<sub>6</sub> was capable of forming ion-channel-like pores at concentrations as low as 10 μM, BAMs 1–3 required 2 to 10-fold higher concentrations to induce transmembrane ion fluctuations (Figure 1c).

We also examined compounds 1–3 for their capability to induce membrane lysis (i.e., rupture of membranes) in the planar lipid bilayers. In these studies, all BAMs were found to require a higher concentration to lyse the membrane compared to BTA-EG<sub>6</sub>, with BAM 1 requiring a 3-fold higher concentration to lyse the membrane and no observed membrane lysis induced by BAM 3 at any of the concentrations tested (i.e., up to 150 μM) (Figure 1c).

In order to evaluate if the structural modifications to BTA-EG<sub>6</sub> correlated with a decrease in toxicity, an MTT cell proliferation assay was performed to compare the toxicity of BAM 1–3 to the parent compound. In this assay, BTA-EG<sub>6</sub> exhibited moderate toxicity to differentiated SH-SY5Y neuroblastoma cells with an IC<sub>50</sub> of 69 μM (Figure 1d, see SI Figure S4 for cell viability versus concentration curves used to estimate IC<sub>50</sub> values). Figure 1d shows that all BAMs 1–3 were significantly less toxic than BTA-EG<sub>6</sub>, with IC<sub>50</sub>'s ranging from 110 to 140 μM. Importantly, the reduced toxicity of these compounds corresponded with the increased concentrations required to lyse membranes. The data in Figure 1 shows that removal of the 6-methyl group was sufficient to reduce both toxicity and membrane lysis activity. Reintroduction of a methyl group to the aniline nitrogen as in BAM2-EG<sub>6</sub> restored cell toxicity and membrane lytic properties. However, replacement of the aniline nitrogen with a sulfur atom in BTA-EG<sub>6</sub> (as in BAM3-EG<sub>6</sub>) led to the least toxic compound in this series, with no membrane lysis observed at concentrations up to 150 μM. These results support a correlation between membrane lysis, pore-forming capabilities, and toxicity of the BAM agents and demonstrate that the small structural changes made to the parent BTA-EG<sub>6</sub> structure can lead to compounds with measurably improved biocompatibility.

In order to evaluate whether 1–3 could bind to aggregated Aβ peptides with similar affinity as BTA-EG<sub>6</sub>, we used a preparation of Aβ (1–42) that mimicked the heterogeneous population of aggregated Aβ species present in the brains of AD patients. This preparation contained ~12% small Aβ oligomers (MW < 15 kDa corresponding to monomers-trimers), ~16% medium-sized oligomers (MW 20–65 kDa corresponding to 5–15 mers), and ~72% soluble protofibrils (MW > 150 kDa corresponding to >30 mers) (see SI Figure S5). We then used a previously reported fluorescence-based binding assay to estimate K<sub>d</sub> values for the association of the BAMs to this preparation of aggregated Aβ (1–42) peptides.<sup>17</sup> All compounds were found to bind Aβ in the mid nanomolar range (Figure 2a, see also SI Figure S6). These binding affinities were comparable to previously reported K<sub>d</sub> values for the binding of BTA-EG<sub>x</sub> to aggregated Aβ (1–42).<sup>17,18</sup>

Since BTA-EG<sub>x</sub> compounds were previously shown to reduce the toxicity of Aβ (1–42) in cells through the formation of protein-resistive coatings on Aβ aggregates,<sup>8,19</sup> we next examined whether BAMs 1–3 also exhibited such cytopro-

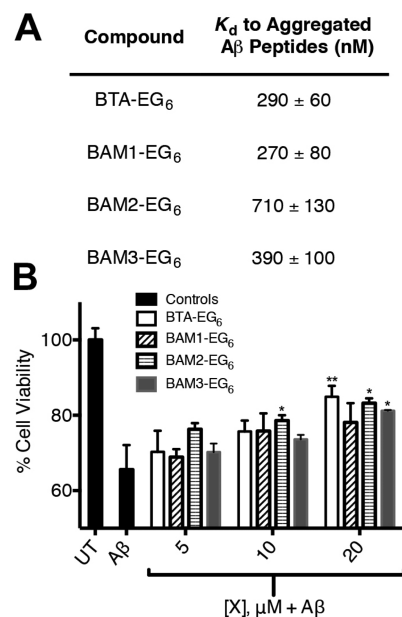


**Figure 2.** Binding of BAM agents to aggregated Aβ and evaluation of cytoprotective properties in SH-SY5Y cells. (A) Dissociation constant K<sub>d</sub> of compounds to aggregated Aβ peptides. (B) Cytoprotective effects of BTA-EG<sub>6</sub> and BAMs 1–3 against aggregated Aβ toxicity (25 μM) in differentiated SH-SY5Y neuroblastoma cells. UT = untreated cells. Data expressed as mean values ± SD, n = 3 or more for each concentration. \*P < 0.05 or \*\*P < 0.01 compared to cells incubated with 25 μM Aβ alone (i.e., in the absence of small molecules).

protective properties. Exposure of differentiated SH-SY5Y cells to 25 μM concentrations of aggregated Aβ (1–42) peptides resulted in a 35% decrease in cell viability (Figure 2a), as determined by an MTT cell proliferation assay. As expected, BAMs 1–3 were capable of reducing the toxicity of Aβ, leading to a dose-dependent trend of increasing cell viability to ~80% at concentrations of 20 μM of compounds in the presence of 25 μM Aβ (Figure 2b).

In order to evaluate the BAMs for their ability to inhibit Aβ-induced oxidative stress, we analyzed the cellular H<sub>2</sub>O<sub>2</sub> levels in the presence of aggregated Aβ with or without the presence of compounds 1–3. Differentiated SH-SY5Y cells were first incubated in the presence of 25 μM aggregated Aβ. After 24 h, we observed a 4-fold increase in cellular H<sub>2</sub>O<sub>2</sub> levels compared to untreated cells (Figure 3). As a positive control, addition of 3-AT, a known catalase inhibitor,<sup>8</sup> to cells also showed about a 4-fold increase in H<sub>2</sub>O<sub>2</sub> levels over the control cells (Figure 3). When cells were treated with aggregated Aβ in the presence of various concentrations (0–40 μM) of BTA-EG<sub>6</sub> or BAMs 1–3, a dose dependent reduction in H<sub>2</sub>O<sub>2</sub> levels was observed for all compounds. Furthermore, the levels of cellular H<sub>2</sub>O<sub>2</sub> when cells were incubated with 25 μM Aβ in the presence of 40 μM concentrations of any of the compounds tested were statistically indistinguishable from control cells (Figure 3). Interestingly, BAM 3 caused a significantly improved reduction of Aβ-induced increase in cellular H<sub>2</sub>O<sub>2</sub>, with statistically significant activity observed at concentrations as low as 1 μM. We hypothesized that this inhibition of Aβ-induced increases in cellular H<sub>2</sub>O<sub>2</sub> levels was due to the capability of the BAM agents to inhibit catalase-Aβ interactions. In order to rule out the possibility that the BAM agents exhibited inherent antioxidant properties that were independent from their capability to bind to aggregated Aβ, we

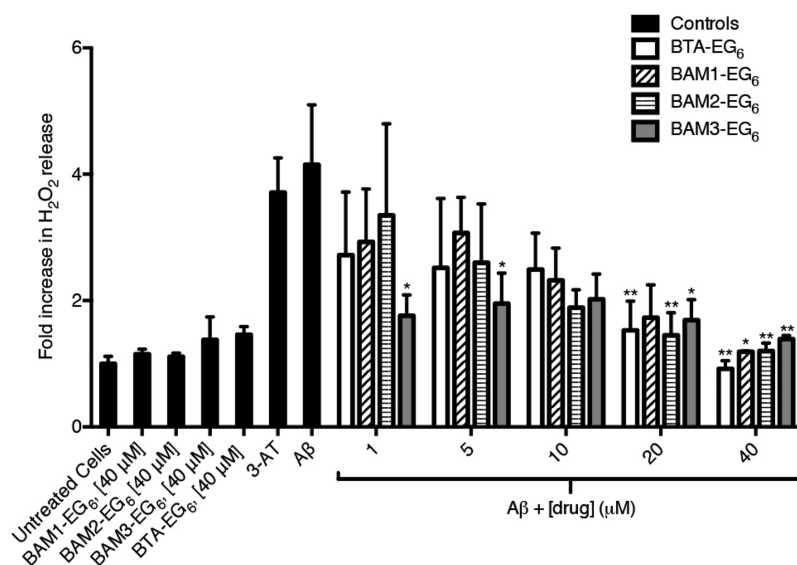


**Figure 3.** Reduction of the  $A\beta$ -induced increase of  $H_2O_2$  release by BTA-EG<sub>6</sub> or BAMs 1–3 in SH-SY5Y cells. Cells treated with  $A\beta$  (25  $\mu M$ ) or 3AT, a catalase inhibitor show an  $\sim 4$ -fold increase in  $H_2O_2$  compared to untreated cells. Cells that were treated with aggregated  $A\beta$  (25  $\mu M$ ) that was preincubated with 1–40  $\mu M$  concentrations of BTA-EG<sub>6</sub> or BAMs 1–3 show a dose-dependent decrease in  $H_2O_2$  release. Cells treated with compounds alone showed no statistical change in  $H_2O_2$  release relative to untreated cells. (\* $P < 0.05$  or \*\* $P < 0.01$  compared to cells treated with 25  $\mu M$   $A\beta$  alone). Data expressed as mean values  $\pm$  SD,  $n \geq 3$  for each concentration.

incubated BAMs 1–3 over 24 h (i.e., the same time course as cellular oxidative stress assay) in the presence of 3 mM  $H_2O_2$  and monitored these reactions for any products from oxidation by mass spectrometry (see the SI for details). We did not observe any oxidation products for any of the BAM agents under these conditions, supporting that the observed decrease in cellular  $H_2O_2$  levels by compounds 1–3 in the presence of  $A\beta$  was likely due to their capability to target aggregated  $A\beta$ .

BTA-EG<sub>6</sub> was previously shown to inhibit catalase- $A\beta$  interactions both in cells and in cell-free assays.<sup>8</sup> In order to confirm that the BAM agents could also inhibit catalase- $A\beta$  interactions, we dosed cells with  $A\beta$  with or without the presence of compounds 1–3 and examined the extent of intracellular colocalization of  $A\beta$  and catalase compared to cells that were treated with  $A\beta$  alone (Figure 4, also see SI Figure S7 for images of control cells and Figure S8 for 2D histograms of colocalization of  $A\beta$  and catalase). This colocalization was determined by fixing the cells after incubation with  $A\beta$  and compounds, fluorescent immunolabeling of  $A\beta$  and catalase, and quantifying colocalization using the Pearson's correlation coefficient (PCC)<sup>20</sup> within the entire three-dimensional volume of the cells. When cells were treated with  $A\beta$ , the PCC for colocalization of  $A\beta$  and catalase was found to be 0.57, indicating a substantial degree of colocalization. However, when treated with BTA-EG<sub>6</sub> or BAMs 1–3, the PCC for  $A\beta$  and catalase reduced to 0.19–0.09 (Figure 4). These results suggest that the tested BAM compounds were indeed capable of reducing the interaction of  $A\beta$  with catalase, with both BAM 1 and BAM 3 showing the highest reduction in colocalization of catalase and  $A\beta$  among the compounds tested. Additionally, while these results do not rule out any effects the BAM compounds may have on cellular uptake of  $A\beta$ , we have previously shown that BTA-EG<sub>4</sub> and BTA-EG<sub>6</sub> did not cause any statistically significant changes in the uptake of aggregated  $A\beta$  peptides in cells.<sup>8</sup> We, therefore, presume that the BAM agents reduce  $A\beta$ -induced increases in  $H_2O_2$  primarily through

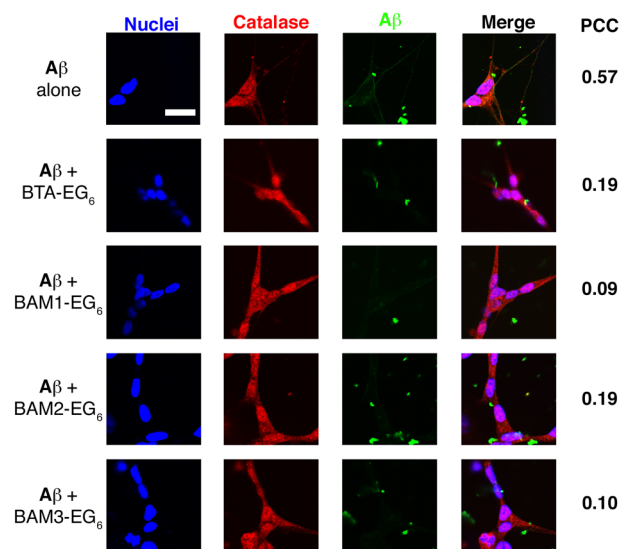


**Figure 4.** Colocalization of aggregated  $A\beta$  (1–42) with catalase in SH-SY5Y cells. Fluorescence micrographs of representative z-slices within a cell illustrate the reduced colocalization of catalase (red) and  $A\beta$  peptides (green) in the presence of 40  $\mu M$  concentrations of the BTA-EG<sub>6</sub> or BAMs 1–3. The nuclei of imaged cells are depicted in blue, and merged images are shown on the right. Scale bar = 20  $\mu m$ .

inhibiting intracellular catalase- $A\beta$  interactions and do not significantly affect cellular uptake of  $A\beta$ .

To further confirm that BAMs 1–3 were able to inhibit catalase- $A\beta$  interactions, we used a previously described semiquantitative ELISA-based assay<sup>19</sup> to evaluate the relative interaction of human catalase with aggregated  $A\beta$  in the presence of BAMs 1–3 or BTA-EG<sub>6</sub>. In this assay, aggregated  $A\beta$  was deposited into wells of a 96-well plate and then incubated with catalase in the presence of increasing concentrations of compound. Results from this assay then reveal the concentrations of small molecules required to observe inhibition of catalase binding to aggregated  $A\beta$  as well



as the maximal extent of the inhibition of binding. We found that all compounds effectively decrease the interaction of catalase and  $A\beta$  at similar concentrations and to a similar extent (Figure 5). These results further support that BAMs 1–3 are capable of forming protein-resistive coatings on aggregated  $A\beta$ .

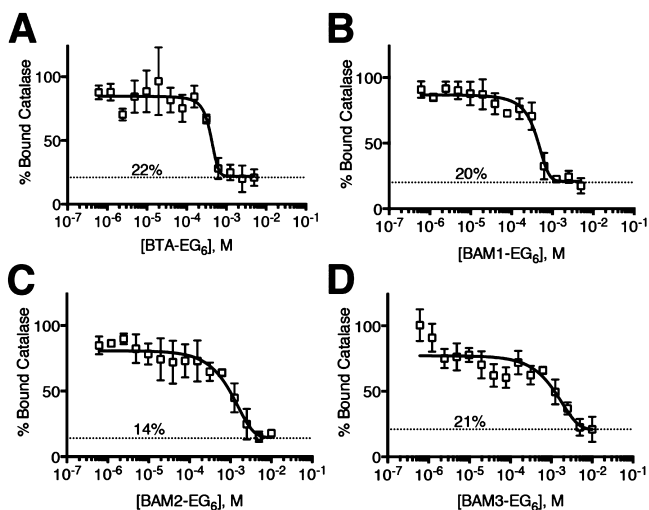


**Figure 5.** Inhibition of catalase- $A\beta$  interactions by BTA-EG<sub>6</sub> and BAMs 1–3. The percentage of bound catalase to  $A\beta$  was decreased in the presence of increasing concentrations of A) BTA-EG<sub>6</sub>, B) BAM1-EG<sub>6</sub>, C) BAM2-EG<sub>6</sub>, and D) BAM3-EG<sub>6</sub>. 100% bound was defined as the amount of catalase bound to  $A\beta$  in the vehicle controls (1% BSA/PBS). Data expressed as mean values  $\pm$  SD,  $n = 3$  for each concentration.

In conclusion, we introduce three benzothiazole amphiphiles that exhibited improved biocompatibility in SH-SY5Y cells compared to BTA-EG<sub>6</sub>. The decreased toxicity of these BAM compounds corresponded with their decreased capability to form ion pores in lipid bilayers and to lyse membranes. Importantly, these BAM compounds were able to 1) bind to aggregated  $A\beta$ , 2) decrease the toxicity of  $A\beta$  in differentiated neuroblastoma cells, 3) decrease  $A\beta$ -induced increases in cellular H<sub>2</sub>O<sub>2</sub> levels, 4) reduce the colocalization of  $A\beta$  and catalase in cells, and 5) inhibit the interaction of catalase and aggregated  $A\beta$  in solution. These results are consistent with the capability of these benzothiazoles to form protein-resistive coatings on aggregated  $A\beta$  and to diminish deleterious interactions between catalase and  $A\beta$  in cells. The capability of the BAM agents to neutralize  $A\beta$  activity makes it possible for catalase to maintain normal cellular levels of H<sub>2</sub>O<sub>2</sub> in an  $A\beta$ -rich environment, leading to reduced toxicity of  $A\beta$  to cells. While the experiments described here focus on the effects of the BAM agents on the interaction of aggregated  $A\beta$  with catalase,  $A\beta$  has been shown to interact with a variety of other cellular proteins.<sup>19,21,22</sup> We have shown previously that molecules such as BTA-EG<sub>6</sub> are capable of inhibiting several proteins from interacting with aggregates comprised of multiple amyloidogenic peptides,<sup>17,19</sup> suggesting that the new BAM agents may be capable of simultaneously inhibiting a variety of protein-amyloid interactions that can cause damage to cells. These new BAM agents, thus, represent an exciting new family of compounds that have potential therapeutic value for treating AD and possibly other amyloid-related diseases. In particular, the new compound BAM3-EG<sub>6</sub> (3) exhibited the greatest biocompatibility and anti- $A\beta$  activity of the compounds tested,

and can serve as a lead candidate for further development of inhibitors of  $A\beta$ -protein interactions as potential therapeutics for AD.

## METHODS

**Materials.** Synthetic  $A\beta(1-42)$  peptide was purchased from PL Lab (Port Moody, Canada). SH-SY5Y human neuroblastoma cells (Product No: CRL-2266) and 3-(4,5-dimethylthiazolyl-2)-2, 5-diphenyltetrazolium bromide (MTT) cell proliferation assay (Product No: 30-1010K) were purchased from American Type Culture Collection (ATCC) (Manassas, VA). The Amplex red hydrogen peroxide kit (# A22188) was from Molecular Probes of Invitrogen Co. and 3-amino-1,2,4-triazole (3AT) (# A8056) was from Sigma-Aldrich. All other chemical reagents were purchased from either Sigma-Aldrich or Fisher and used as is unless otherwise stated.

**Planar Lipid Bilayer Studies.** The procedure for PLB recordings was performed as previously described.<sup>13</sup> Briefly, planar lipid bilayers were prepared from a solution of 20 mg/mL 1,2-diphytanoyl-*sn*-glycero-3-phosphatidylcholine (Di-PhyPC) in decane by the painting method. Both compartments of the recording chamber were filled with an electrolyte solution containing 1 M CsCl and 10 mM HEPES buffer (pH = 7.4). Currents were recorded with a filter cutoff frequency of 5 kHz and a sampling frequency of 25 kHz using a Geneclamp-500 amplifier (Axon instruments), and further filtered at 200 Hz using a Gaussian low-pass filter for analysis. For this experiment, we defined the minimum concentration of pore formation to be the concentration where the frequency of observed channel events was greater than 0.05 per minute and where we observed at least 1 event per 20 min recording.

**MTT Cell Proliferation Assay.** SH-SY5Y neuroblastoma cells were differentiated as previously described.<sup>23</sup> Briefly, cells were plated at a density of 50,000 cells/well in 100  $\mu$ L of 1:1 EMEM and Ham's F12, supplemented with 10% FBS and without phenol red. After adhering overnight, medium was replaced with differentiating medium by addition of 10  $\mu$ M *all-trans*-retinoic acid (RA). Medium with RA was replaced every 2 days for 8 days total. After 8 days, the media was removed and 100  $\mu$ L of new, RA-free medium containing various concentrations of either BTA-EG<sub>6</sub> or BAMs-EG<sub>6</sub> with final concentrations (0–500  $\mu$ M). Cells were exposed to these solutions for 24 h at 37 °C. MTT cell viability assay was then used to determine cell viability. All results are presented as percent reduction of MTT relative to untreated cells (100% viability).

**Cytoprotection of Differentiated SH-SY5Y Neuroblastoma Cells.** Differentiated SH-SY5Y cells were exposed to solutions containing a final concentration of 25  $\mu$ M  $A\beta$  and various concentrations of the BTA-E<sub>6</sub> and BAMs (0–20  $\mu$ M), dissolved in RA-free medium for 24 h at 37 °C. The Supporting Information describes the details of pretreatment of all  $A\beta$  samples. Note: the concentration of aggregated  $A\beta$  reported here refers to the  $A\beta$  concentration if all  $A\beta$  would be present in monomeric, dissolved form. The MTT reagent (10  $\mu$ L of the solution from the commercial kit) was then added and the cells were incubated for 3 additional hours. The cells were subsequently solubilized with detergent reagent (100  $\mu$ L of the solution from the commercial kit) and incubated at room temperature overnight. The cell viability was determined by measuring the absorbance at 570 nm using a Spectramax 190 microplate reader (Molecular Devices). All results were expressed as percent reduction of MTT relative to untreated

controls (defined as 100% viability), and the average absorbance value for each treatment was normalized to the absorbance reading of wells containing only media, MTT reagent, and detergent reagent.

**Measurement of the Binding Affinity of BTA-EG<sub>6</sub> and BAMs to Aggregated A $\beta$  (1–42) Peptides.** Binding of compounds to aggregated A $\beta$  (1–42) was measured according to a previously described assay.<sup>17</sup> Briefly, 200  $\mu$ L of various concentrations of BTA/BAM compounds in PBS were incubated in the absence or presence of 10  $\mu$ g of preaggregated A $\beta$  (total volume 220  $\mu$ L). Solutions were allowed to equilibrate overnight at room temperature. Samples were then centrifuged at 16,000g for 20 min at 4 °C. The supernatants were removed, and the pellet was resuspended in 220  $\mu$ L of fresh PBS. Fluorescence of the bound molecule was determined using a spectrofluorometer (Photon Technology International, Inc., Birmingham, NJ). Each experiment was repeated at least three times and error bars denote standard deviation from the mean. Graphs shown in Figures S6 were fit using the following one-site specific binding algorithm to determine  $K_d$ :  $Y = B_{max} \times X / (K_d + X)$ , where  $X$  is the concentration of small molecule,  $Y$  is the specific binding intensity, and  $B_{max}$  is the apparent maximal observable fluorescence upon binding to A $\beta$ . Data was processed using Origin 7.0 (MicroCal Software, Inc., Northampton, MA).

**Assay for Hydrogen Peroxide Release from Differentiated SH-SY5Y Neuroblastoma Cells.** Cells were differentiated as previously mentioned in DMEM without phenol red and supplemented with 10% FBS, 4 mM L-glutamine, and 10  $\mu$ M RA for 8 days. Solutions of A $\beta$  aggregates with and without compounds in RA-free medium were incubated with the cells for 24 h. Hydrogen peroxide release was determined by adding 20  $\mu$ L/well of a solution containing 250  $\mu$ M Amplex red reagent and 0.5 U/mL Horseradish Peroxidase (HRP) dissolved in complete medium. After 30 min, the absorbance at 560 nm was measured. For controls, cells were incubated with 40  $\mu$ M of each compound alone; a positive control of 20 mM 3AT (a catalase inhibitor) was also added in each experiment, with no observed effect of compounds on 3AT-induced increases in H<sub>2</sub>O<sub>2</sub> levels in cells (data not shown). All experiments were done at least in triplicate, and control wells of medium alone were used for normalization of all samples.

**Confocal Microscopy of the Cellular Colocalization of A $\beta$  and Catalase.** SH-SY5Y cells were cultured on 35 mm dishes (MatTek) and incubated overnight in a 1:1 mixture of EMEM and Ham's F12 supplemented with 10% FBS. The growth medium was removed, and solutions containing aggregated A $\beta$  (5  $\mu$ M) with or without compounds (40  $\mu$ M) were added in fresh medium. The cells were incubated for 12 h (37 °C, 5% CO<sub>2</sub>). To visualize the colocalization of aggregated A $\beta$  with catalase, the cells were rinsed (3 $\times$ , PBS), fixed with 4% paraformaldehyde in PBS (pH 7.4), and permeabilized with 0.25% Triton-X in PBS. Cells were then blocked with 10% goat serum/PBS (1 h, RT) and then incubated with primary antibodies: mouse anti-A $\beta$  (6E10, Covance) and rabbit anti-catalase (Abcam) antibody on a shaker at 4 °C overnight. To detect the primary antibodies, the following fluorescently labeled secondary antibodies were used: TRITC-conjugated goat antimouse (Jackson ImmunoResearch) and an Alexa Fluor 488-conjugated goat-anti rabbit (Jackson ImmunoResearch) and incubated in the dark (1 h, RT). Matteks were then rinsed (3 $\times$ , PBS with the last rinse containing NucBlue fixed

cell stain, Molecular Probes) and then mounted using Dako fluorescent mounting medium (Product # S3023) and let dry before imaging with a Olympus FV1000 spectral deconvolution confocal system equipped with an Olympus IX81 inverted microscope. The colocalization was visualized, and Pearson's correlation coefficient (PCC) of the entire three-dimensional volume of the cell was determined using ImageJ. The images shown in Figure 4 are fluorescence micrographs of representative z-slices within cells.

**Decrease in Catalase-A $\beta$  Binding Using Small Molecules.** The inhibition of catalase-A $\beta$  interactions by small molecules was determined by a previously described protocol.<sup>19</sup> Briefly, the wells of a 96-well plate were coated with a solution of aggregated A $\beta$  in PBS (2h, 1.3  $\mu$ M). After removal of solutions containing excess A $\beta$ , all wells were blocked with 1% BSA/PBS (1 h), washed with PBS, and then incubated for 2 h with a human catalase solution (0.20  $\mu$ M, in 1% BSA/PBS buffer). After removal of solutions containing excess catalase, solutions of various concentrations of small molecules in 1% BSA/PBS buffer were incubated in the wells for 12 h. Wells were then washed with 1% BSA/PBS and incubated for 1 h with monoclonal mouse anti-catalase IgG (clone 1A1, 2.2 nM in 1% BSA/PBS). Excess solution was removed; wells were washed with PBS and then incubated for 45 min with an alkaline phosphatase conjugated polyclonal secondary rabbit IgG (antimouse IgG, 6.8 nM in 1% BSA/PBS). The relative amount of secondary IgG bound was quantified by adding a solution containing *p*-nitrophenyl phosphate (NPP, 2.7 mM, in 0.1 M diethanol amine/0.5 mM magnesium chloride, pH 9.8) to each well. The enzymatic hydrolysis reaction of NPP by alkaline phosphatase was stopped after 45 min by addition of 0.25 N sodium hydroxide. The concentration of *p*-nitrophenoxide was then quantified at A<sub>405</sub> using a UV-vis microplate reader (Molecular Devices). Each data point from this assay represents the average of at least three independent experiments. Error bars represent standard deviations. Graphs were normalized, plotted, and fitted with the sigmoidal curve fitting option in Prism 6.0 (GraphPad Software Inc.).

## ■ ASSOCIATED CONTENT

### 📄 Supporting Information

The Supporting Information is available free of charge on the ACS Publications website at DOI: 10.1021/acchemneur-0.6b00085.

Synthetic procedures along with <sup>1</sup>H NMR, <sup>13</sup>C NMR, and MS data, binding curves, details of A $\beta$  preparation, current versus time traces for electrical recordings of the BAMs in planar lipid bilayers, and additional images supporting colocalization of A $\beta$  and catalase (PDF)

## ■ AUTHOR INFORMATION

### Corresponding Author

\*Phone: 858-534-6006. Fax: 858-534-4554. E-mail: jerryyang@ucsd.edu.

### Author Contributions

J.L.C., M.M. and J.Y. designed the research and analyzed the data. J.L.C., T.S.C, H.L., P.P. executed the experiments. J.L.C. and J.Y. wrote the manuscript.

### Funding

This work was partially supported by the UCSD Alzheimer's Disease Research Center (NIH 3P50 AG005131).

## Notes

The authors declare no competing financial interest.

## ACKNOWLEDGMENTS

We would like to thank Jennifer Santini for use of the UCSD School of Medicine Microscopy Core, which is supported by NIH grant P30 NS04710. We would also like to thank Dr. Su and the UCSD Chemistry and Biochemistry Molecular MS Facility.

## REFERENCES

- (1) Finkel, T., and Holbrook, N. J. (2000) Oxidants, oxidative stress and the biology of ageing. *Nature* 408, 239–247.
- (2) Pohanka, M. (2014) Alzheimer's disease and oxidative stress: a review. *Curr. Med. Chem.* 21, 356–364.
- (3) Nunomura, A., Perry, G., Aliev, G., Hirai, K., Takeda, A., Balraj, E. K., Jones, P. K., Ghanbari, H., Wataya, T., Shimohama, S., Chiba, S., Atwood, C. S., Petersen, R. B., and Smith, M. A. (2001) Oxidative damage is the earliest event in Alzheimer disease. *J. Neuropathol. Exp. Neurol.* 60, 759–767.
- (4) Barnham, K. J., Masters, C. L., and Bush, A. I. (2004) Neurodegenerative diseases and oxidative stress. *Nat. Rev. Drug Discovery* 3, 205–214.
- (5) Butterfield, D. A., Drake, J., Pocernich, C., and Castegna, A. (2001) Evidence of oxidative damage in Alzheimer's disease brain: central role for amyloid  $\beta$ -peptide. *Trends Mol. Med.* 7, 548–554.
- (6) Uttara, B., Singh, A. V., Zamboni, P., and Mahajan, R. T. (2009) Oxidative stress and neurodegenerative diseases: a review of upstream and downstream antioxidant therapeutic options. *Curr. Neuropharmacol.* 7, 65–74.
- (7) Wang, X., and Michaelis, E. K. (2010) Selective neuronal vulnerability to oxidative stress in the brain. *Front. Aging Neurosci.* 2, 12.
- (8) Habib, L. K., Lee, M. T. C., and Yang, J. (2010) Inhibitors of catalase-amyloid interactions protect cells from beta-amyloid-induced oxidative stress and toxicity. *J. Biol. Chem.* 285, 38933–38943.
- (9) Behl, C., Davis, J. B., Lesley, R., and Schubert, D. (1994) Hydrogen peroxide mediates amyloid beta protein toxicity. *Cell* 77, 817–827.
- (10) Song, J. M., DiBattista, A. M., Sung, Y. M., Ahn, J. M., Turner, R. S., Yang, J., Pak, D. T. S., Lee, H.-K., and Hoe, H.-S. (2014) A tetra(ethylene glycol) derivative of benzothiazole aniline ameliorates dendritic spine density and cognitive function in a mouse model of Alzheimer's disease. *Exp. Neurol.* 252, 105–113.
- (11) Capule, C. C., Brown, C., Olsen, J. S., Dewhurst, S., and Yang, J. (2012) Oligovalent amyloid-binding agents reduce SEVI-mediated enhancement of HIV-1 infection. *J. Am. Chem. Soc.* 134, 905–908.
- (12) Megill, A., Lee, T., Dibattista, A. M., Song, J. M., Spitzer, M. H., Rubinshtein, M., Habib, L. K., Capule, C. C., Mayer, M., Turner, R. S., Kirkwood, A., Yang, J., Pak, D. T. S., Lee, H.-K., and Hoe, H.-S. (2013) A Tetra(Ethylene Glycol) Derivative of Benzothiazole Aniline Enhances Ras-Mediated Spinogenesis. *J. Neurosci.* 33, 9306–9318.
- (13) Prangkio, P., Rao, D. K., Lance, K. D., Rubinshtein, M., Yang, J., and Mayer, M. (2011) Self-assembled, cation-selective ion channels from an oligo(ethylene glycol) derivative of benzothiazole aniline. *Biochim. Biophys. Acta, Biomembr.* 1808, 2877–2885.
- (14) Ma, Q., and Lu, A. Y. H. (2011) Pharmacogenetics, pharmacogenomics, and individualized medicine. *Pharmacol. Rev.* 63, 437–459.
- (15) Prangkio, P., Yusko, E. C., Sept, D., Yang, J., and Mayer, M. (2012) Multivariate analyses of amyloid-beta oligomer populations indicate a connection between pore formation and cytotoxicity. *PLoS One* 7, e47261.
- (16) Cifelli, J. L., Dozier, L., Chung, T., Patrick, G. N., and Yang, J. Benzothiazole Amphiphiles Promote the Formation of Dendritic Spines in Primary Hippocampal Neurons. *J. Biol. Chem.*, published online March 28, 2016. DOI: 10.1074/jbc.M115.701482.
- (17) Olsen, J. S., Brown, C., Capule, C. C., Rubinshtein, M., Doran, T. M., Srivastava, R. K., Feng, C., Nilsson, B. L., Yang, J., and Dewhurst, S. (2010) Amyloid-binding small molecules efficiently block SEVI (semen-derived enhancer of virus infection)- and semen-mediated enhancement of HIV-1 infection. *J. Biol. Chem.* 285, 35488–35496.
- (18) Capule, C. C., and Yang, J. (2012) Enzyme-linked immunosorbent assay-based method to quantify the association of small molecules with aggregated amyloid peptides. *Anal. Chem.* 84, 1786–1791.
- (19) Inbar, P., Li, C. Q., Takayama, S. A., Bautista, M. R., and Yang, J. (2006) Oligo(ethylene glycol) derivatives of thioflavin T as inhibitors of protein-amyloid interactions. *ChemBioChem* 7, 1563–1566.
- (20) Bolte, S., and Cordelières, F. P. (2006) A guided tour into subcellular colocalization analysis in light microscopy. *J. Microsc.* 224, 213–232.
- (21) Stains, C. I., Mondal, K., and Ghosh, I. (2007) Molecules that target beta-amyloid. *ChemMedChem* 2, 1674–1692.
- (22) Kim, T., Vidal, G. S., Djuricic, M., William, C. M., Birnbaum, M. E., Garcia, K. C., Hyman, B. T., and Shatz, C. J. (2013) Human LILRB2 is a  $\beta$ -amyloid receptor and its murine homolog PirB regulates synaptic plasticity in an Alzheimer's model. *Science* 341, 1399–1404.
- (23) Datki, Z., Juhász, A., Gálfy, M., Soós, K., Papp, R., Zádori, D., and Penke, B. (2003) Method for measuring neurotoxicity of aggregating polypeptides with the MTT assay on differentiated neuroblastoma cells. *Brain Res. Bull.* 62, 223–229.